


# Chemical Synthesis of Innovative Silver Nanohybrids with Synergistically Improved Antimicrobial Properties

Jianhua Yan<sup>1</sup>, Qifei Wang<sup>1,2</sup>, Junlin Yang<sup>2</sup>, Paige Rutter<sup>1</sup>, Malcolm Xing<sup>3</sup>, Bingyun Li <sup>1</sup>

<sup>1</sup>Department of Orthopaedics, School of Medicine, West Virginia University, Morgantown, WV, 26506, USA; <sup>2</sup>Spine Center, Xin Hua Hospital Affiliated to Shanghai Jiao Tong University School of Medicine, Shanghai, People's Republic of China; <sup>3</sup>Department of Mechanical Engineering, University of Manitoba, Winnipeg, R3T2N2, Canada

Correspondence: Bingyun Li, Department of Orthopaedics, School of Medicine, West Virginia University, 64 Medical Center Drive, Morgantown, WV, 26506, USA, Tel +1 681-285-5956; +1 304-293-1075, Fax +1 304-293-7070, Email bili@hsc.wvu.edu

**Background:** The wide use of antibiotics has created challenges related to antibiotic-resistant bacteria, which have been increasingly found in recent decades. Antibiotic resistance has led to limited choices of antibiotics. Multiple old antimicrobial agents have high antimicrobial properties toward bacteria, but they unfortunately also possess high toxicity toward humans. For instance, silver (Ag) compounds were frequently used to treat tetanus and rheumatism in the 19th century and to treat colds and gonorrhea in the early 20th century. However, the high toxicity of Ag has limited its clinical use.

**Purpose:** We aimed to reformulate Ag to reduce its toxicity toward human cells like osteoblasts and to optimize its antimicrobial properties.

**Results:** Ag, an old antimicrobial agent, was reformulated by hybridizing nanomaterials of different dimensions, and silver nanoparticles (AgNPs) of controllable sizes (95–200 nm) and varying shapes (cube, snowflake, and sphere) were synthesized on carbon nanotubes (CNTs). The obtained AgNP-CNT nanohybrids presented significantly higher killing efficacy against *Staphylococcus aureus* (*S. aureus*) compared to AgNPs at the same molar concentration and showed synergism in killing *S. aureus* at 0.2 and 0.4 mM. AgNPs presented significant osteoblast toxicity; in contrast, AgNP-CNT nanohybrids demonstrated significantly enhanced osteoblast viability at 0.04–0.8 mM. The killing of *S. aureus* by AgNP-CNT nanohybrids was fast, occurring within 15 min.

**Conclusion:** Ag was successfully reformulated and Ag nanohybrids with various AgNP shapes on CNTs were synthesized. The nanohybrids presented significantly enhanced antimicrobial properties and significantly higher osteoblast cell viability compared to AgNPs, showing promise as an innovative antimicrobial nanomaterial for a broad range of biomedical applications.

**Keywords:** silver nanoparticle, nanohybrid, antimicrobial, cytotoxicity, reformulation, antibiotic resistance

## Introduction

In recent decades, antibiotic resistance has been making infection treatment very difficult.<sup>1</sup> Antibiotics have been credited for reducing infection; however, extensive use of antibiotics has also led to antibiotic resistance, a grave challenge in patient care. Approximately 38.7–50.9% of the bacteria resulting in surgery-related infections are found to be resistant to conventional antibiotics.<sup>2,3</sup> From 1997 to 2006, infections from antibiotic-resistant bacteria increased by 359% in the USA,<sup>4</sup> and antibiotic-resistant bacteria led to over 2.8 million infections as well as 35,000+ deaths every year.<sup>5</sup> Unfortunately, fewer and fewer new antibiotics are being approved or are in development; for example 30 and 17 new antibiotics were approved by FDA during 1983–1992 and 1993–2002, respectively, while only 7 were approved during 2003–2012.<sup>6</sup>

Reformulating or repurposing “old” antimicrobial agents has recently attracted significant interest. Multiple old antimicrobial agents have high antimicrobial properties toward bacteria, but they unfortunately also possess high toxicity toward humans, thereby leading to delayed wound healing and other side effects. For instance, silver (Ag) compounds,

especially Ag nitrate and sulfadiazine, were frequently used to treat tetanus and rheumatism in the 19th century and to treat colds and gonorrhea in the early 20th century.<sup>7</sup> It is reported that Ag nanoparticles (AgNPs) and Ag compounds present broad-spectrum antimicrobial properties against various microorganisms like Gram-positive and Gram-negative bacteria including antibiotic-resistant ones (eg, methicillin-resistant *Staphylococcus aureus* or MRSA), viruses, fungi, and protozoa.<sup>8–16</sup> Ag metals and compounds also have antimicrobial properties against biofilms and intracellular bacteria.<sup>17,18</sup> AgNPs or Ag compounds may provoke microbial resistance,<sup>19,20</sup> although that is less likely compared to conventional antibiotics, since Ag's multilevel antimicrobial modes, including binding to essential cellular structure elements and interfering with the bacterial cell integrity and its energy production and conservation,<sup>21</sup> ensure that resistance may not be easily acquired by simple mutations. For instance, no evidence of Ag resistance was presented in a large collection (876 strains) of clinical *Staphylococcus aureus* (*S. aureus*) isolates and no reduction in Ag susceptibility was observed upon extended passages (eg, 42 days).<sup>22</sup> However, Ag and Ag compounds have significant toxicity toward humans and their use has markedly declined for the last 50 years.<sup>23</sup> Currently, the use of Ag and Ag compounds has been limited by their host toxicity primarily to topical treatments such as dressings in wound care. In the literature, composites of AgNPs and carbon nanotubes (CNTs) have attracted interest recently and a few different composites have been reported.<sup>24–31</sup> For instance, Oluwalowo et al found that composites of AgNPs and CNTs led to significantly improved electrical and thermal conductivity compared to AgNPs or CNTs alone, while no other properties were reported.<sup>24</sup> Zhao et al prepared interesting, stretchable, and printable electronics with high electrical conductivity.<sup>25</sup> Takei et al synthesized composite films of AgNPs and CNTs with excellent bendability and high strain sensitivity.<sup>26</sup> However, AgNP-CNT nanocomposites with well distributed, highly packed AgNPs on CNTs have not been achieved. Their potential for biomedical applications has not been well studied, and the potential synergistic antimicrobial properties have never been reported.

In this study, we synthesized Ag nanohybrids with reduced host toxicity so that previously “old” toxic antimicrobial agents like Ag could potentially find new uses to prevent and treat infections and to have broad antimicrobial applications. We hypothesized that nanohybrids of antimicrobial nanomaterials with different dimensions, such as spherical nanoparticles (zero dimension or 0D) and long nanofibers (one dimension or 1D), could lead to enhanced antimicrobial properties and reduced toxicity toward human cells. Such nanohybrids may also have reduced potential to develop resistance as compared to individual antimicrobial components. AgNPs with different shapes and sizes were synthesized on CNTs, and their antimicrobial activity and cytotoxicity toward human cells at various concentrations were investigated. CNTs have low antibacterial activity based on the contact mechanism and destruction of a bacterial cell wall. CNTs were first treated with nitric acid and hydrogen peroxide to create the surface functional group of –OH. This functional group (ie, –OH) was chelated with Ag-ions, which were next reduced to form AgNPs with varying morphologies (cube, snowflake, or sphere) and different sizes (95–200 nm) on CNTs. The synthesized nanohybrids (ie, AgNP-CNT) were characterized using scanning electron microscopy (SEM), their antimicrobial properties were assessed against *S. aureus*, and their cytotoxicity was evaluated using human osteoblast cells. The results showed that AgNP-CNT nanohybrids were effective against bacteria but had low potential for killing human cells.

## Materials and Methods

### Materials

All chemical materials including silver nitrate (AgNO<sub>3</sub>), nitric acid, hydrogen peroxide (H<sub>2</sub>O<sub>2</sub>), multiwalled CNTs (5–9 μm long and 110–170 nm in diameter), ammonia aqueous solution, dextrose aqueous solution, and sodium hydroxide (NaOH) were from Sigma Aldrich Co., Ltd. *S. aureus* was obtained from the chronic wound of a patient at WVUMedicine (Morgantown, WV, US). Human osteoblast cells (CRL-11226) were purchased from ATCC (Manassas, VA, US). Tryptic soy broth (TSB) was obtained from Becton, Dickinson and Company. The use of these materials to prepare and assess AgNP-CNT nanohybrids is presented in Figure 1.

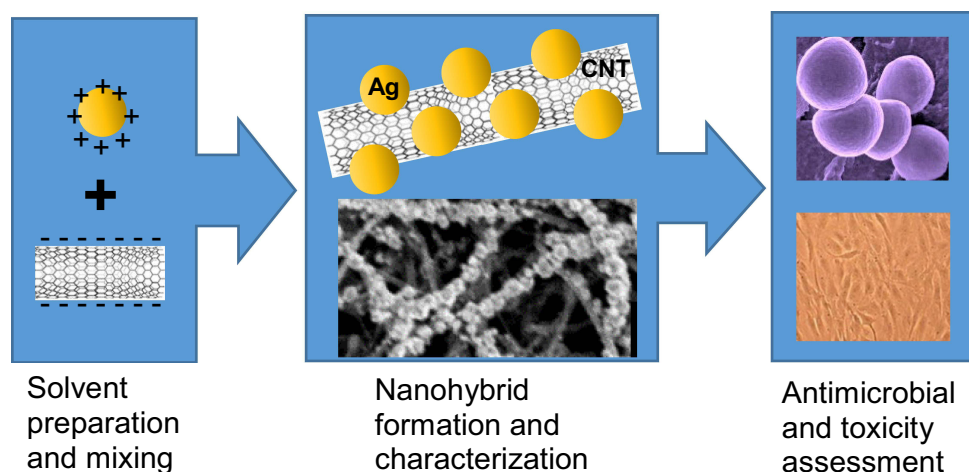
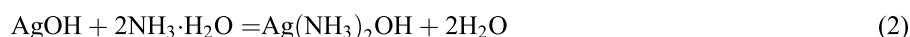


**Figure 1** Schematic diagram presenting the preparation and assessment of AgNP-CNT nanohybrids.

## Synthesis of AgNP-CNT Nanohybrids

Two steps were taken to prepare AgNP-CNT nanohybrids. In the first step, fresh Tollens reagent was prepared. Fifteen-milliliter  $\text{AgNO}_3$  solution (0.2 M) was added into a 100-mL glass bottle with a stirring bar and heated on a hot plate (70 °C). Then, a 7 M ammonia aqueous solution was dropwise added until brown precipitates formed and subsequently disappeared under constant stirring. The two-step chemical reactions are as follows:



Next, 7.5 mL NaOH aqueous solution (1.6 M) was added to the bottle and black precipitates were observed. Ammonia aqueous solution was dropwise added again until the solution became colorless, and Tollens reagent was prepared for subsequent use. In the second step, AgNPs were synthesized based on a silver-mirror reaction and were hybridized with CNTs. Specifically, multiwalled CNTs were functionalized (ie, CNT-OH) as we previously reported,<sup>32,33</sup> and then 150 mg of the functionalized CNTs was immersed in the Tollens reagent at 70 °C for 30 min to let -OH groups chelate with Ag-ions. Next, 3 mL dextrose aqueous solution (0.5 M) was poured into the above solution. The chemical reaction equation is shown below:



The supernatant was decanted and the reaction products were rinsed with distilled water and ethanol. The obtained AgNP-CNT nanohybrids were placed into a vacuum oven under 80 °C for 24 h. Control pure AgNPs were synthesized by substituting CNTs with a copper substrate in the aforementioned process.

## Characterization of AgNPs and AgNP-CNT Nanohybrids

A Hitachi S4700F scanning electron microscope (SEM, Clarksburg, MD, US) with energy-dispersive X-ray spectroscopy (EDX) capability was used to examine the samples. The sizes of AgNPs were evaluated by averaging 40 particles. X-ray diffraction (XRD) data were obtained using a PANalytical X-ray diffractometer and an X-ray generator (40 kV, 20 mA) with CuK radiation (1.54 Å) from 10° to 80° at a scanning speed of 10° per min.

## Tests for Antimicrobial Activity

*S. aureus* was grown in sheep blood agar (Remel-ThermoFisher, San Diego, CA, US), cultured under aerobic conditions at 37 °C overnight, and used for antimicrobial tests, similar to our previous studies.<sup>18,34</sup> Three colonies were added to 5 mL TSB which was then incubated at 37 °C for 16 h. The bacteria with mid logarithmic phase were obtained by adding

100  $\mu\text{L}$  of the inoculum to 20 mL TSB followed by incubation at 37 °C. After shaking for 2 h, 10 mL of the new inoculum was placed in a 15 mL tube and centrifuged under 4 °C at 3750 rpm for 10 min. The supernatant was removed and 10 mL of phosphate buffered saline+ or PBS+ (with Ca and Mg) was added into the tube and thoroughly vortexed to dissolve the pellet. The final concentration of *S. aureus* was adjusted to  $3 \times 10^5$  CFU/mL. The antimicrobial experiments were carried out with 1 mL medium comprised of *S. aureus* and different concentrations of AgNP-CNT; the level of Ag was assessed using inductively coupled plasma-mass spectrometric analysis (ICP-MS) after dissolving samples in nitric acid (70%). CNTs and silver nitrate were tested as positive controls. The samples, including the controls, were incubated for 30 min at 37 °C in a reciprocal shaking bath. After diluting, samples were taken, plated using the drop plate method, and 5% sheep blood agar plates were used. First, a sheep blood agar plate was sectioned into six parts, a drop (20  $\mu\text{L}$ ) of bacterial sample was plated on each part, and the plate was inverted and incubated (37°C, 24 h).

## Tests for Cell Viability

The cell viability of different concentrations of AgNP-CNT on human osteoblast cells was determined using our previous similar protocols.<sup>35</sup> The mitochondrial dehydrogenase activity with MTT assay was carried out. Human osteoblast cells were cultured at 37 °C and fetal bovine serum or FBS (10%) and nonessential amino acids G418 (1%) with humidified CO<sub>2</sub> (5%) were used. The medium was refreshed every 2 days. The preparation of cells is described as follows: first, the stock cell concentration of  $3 \times 10^5$  cells/mL was prepared, and 100  $\mu\text{L}$  of the cells was added to each well ( $3.0 \times 10^4$  cell/well) in a 96-well plate. The cells were cultured for 24 h to allow them to adhere to the wells. The viability tests were conducted as follows: cells were cultured in triplicate with various levels of AgNP-CNT at 37 °C and 5% CO<sub>2</sub>. Cells cultured in fresh medium were used as negative controls. CNTs, AgNPs, and silver nitrate samples were also run. After culturing for 2 h, MTT was dissolved in PBS at 5 mg/mL. The wells were washed, and 100  $\mu\text{L}$  un-supplemented media (no FBS or antibiotics) was added to each well with 10  $\mu\text{L}$  MTT reagent. Samples were then cultured for 2 h. The formation of formazan crystals was checked with a microscope and dimethyl sulfoxide (DMSO, non-sterile, 150  $\mu\text{L}$  for each well) was used to dissolve the formazan crystals. The absorbance at 570 nm was obtained and compared with the control group at each time point and expressed as a percentage.

## Statistical Analyses

Values of percent killing and osteoblast cell viability were calculated as means  $\pm$  standard deviations. Differences in bacterial percent killing and osteoblast cell viability of various treatments were analyzed; JMP-V9 (SAS, Cary, NC) statistical software was applied. Student's *t*-test was used to compare data between any two groups, and one-way ANOVA was applied to compare data among three or more groups followed by Tukey's honestly significant difference test. A *t*-test-based contrast analysis was also used for possible synergistic analysis.  $P < 0.05$  was considered to be statistically significant.

## Results

### Materials Synthesis and Characterization

In this study, we used the classic silver-mirror reaction to synthesize silver NPs and AgNP-CNT nanohybrids. The CNTs were characterized with transmission electron microscopy and X-ray photoelectron spectroscopy (Figures S1 and S2), and their surface element content was obtained (see Supplementary Information Table S1). The multiwalled CNTs used were functionalized using our previous protocols.<sup>32,33</sup> The reactions related to the applied silver-mirror reactions were stoichiometric reactions; by controlling the proportion of reactants, the corresponding design results were obtained. The reactions were stopped immediately once the reactants were consumed, and the uniformity of Ag-loading on CNTs was mainly controlled by the reaction time.

AgNP-CNT nanohybrids with a variety of AgNP morphologies were synthesized under different reaction conditions. Sphere-shaped AgNPs were prepared onto CNTs when the concentration of the dextrose solution was 0.5 M (Figure 2a). Snowflake and cube-shaped AgNPs on CNT surfaces were obtained when the dextrose solution was reduced to 0.25 M and 0.125 M, respectively (Figure 2b and c). During the chemical synthesis of AgNP-CNT, the AgNPs were produced

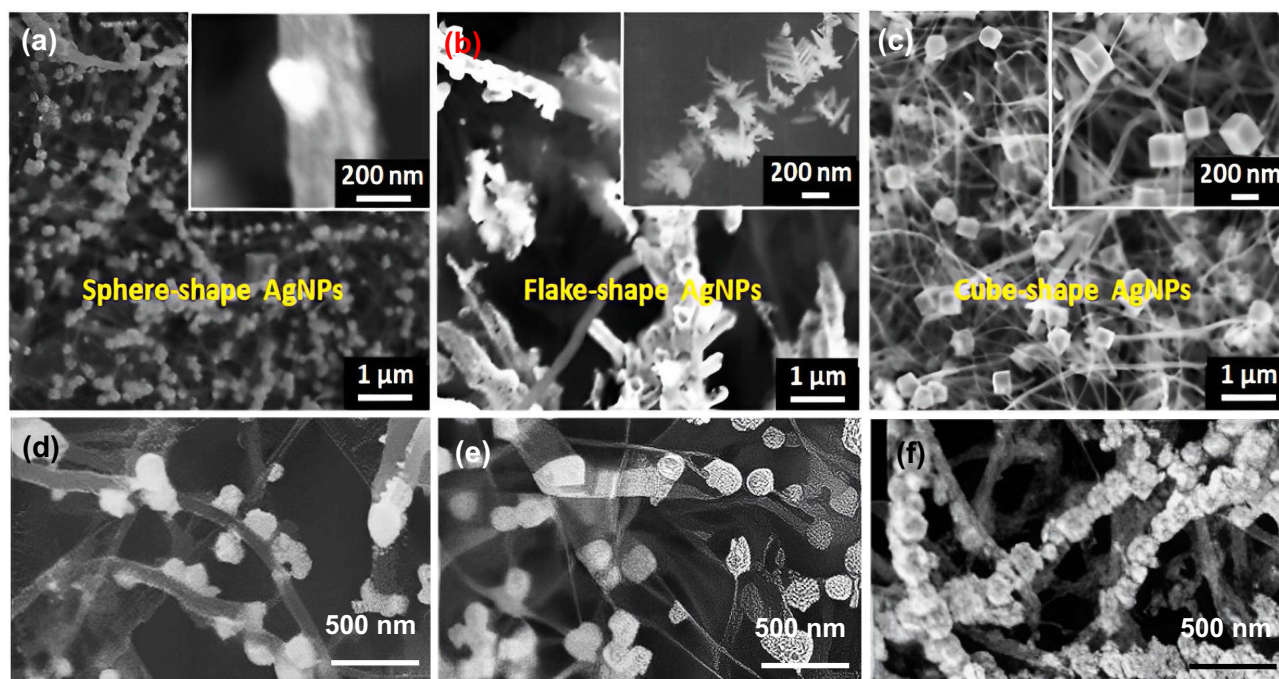


**Figure 2** Material characterization of AgNP-CNT nano hybrids. By maintaining the reaction time of reaction 3 at 60s but decreasing the concentration of dextrose solution from 0.5 M to 0.25 M and further to 0.125 M, the synthesized AgNPs presented (a) sphere-shape, (b) snowflake, and (c) cube-shape. By keeping the concentration of dextrose solution as 0.5 M but increasing the reaction time from (d) 15s to (e) 30s and further to (f) 60s, the amount of AgNPs formed increased correspondingly. The insets show the detailed morphologies of AgNPs.

through the reduction of Ag-ions that chelated onto CNTs. When concentration of the dextrose solution used was low, Ag-atoms tended to crystallize via heterogeneous nucleation which led to formation of cube-shaped AgNPs. Increasing the concentration of dextrose solution resulted in AgNPs growing along the favorable crystallographic directions to form sphere-shaped AgNPs. Meanwhile, the sizes of AgNPs varied with different shapes. The sphere-shaped AgNPs had the smallest average size of  $\sim 95$  nm, while the cube-shaped AgNPs had the largest average size of  $\sim 200$  nm. The sphere-shaped AgNPs, which had the smallest particle size and the largest specific surface area, may present the best antimicrobial effects, and were further optimized and studied for antimicrobial and toxicity properties.

The next step was to optimize the distribution of AgNPs on CNTs. A uniform distribution of AgNPs on CNT surfaces would be expected to maximize the antimicrobial properties of AgNP-CNT nano hybrids. As shown in Figure 2d–f, we tuned the formation of AgNPs on CNT surfaces by changing the reaction time for reaction 3. The density of AgNPs formed on CNT surfaces increased substantially with increasing reaction time. At a reaction time of 15 or 30s (Figure 2d and e), an insufficient amount of AgNPs was formed on the CNT surfaces. When increasing the reaction time to 60s (Figure 2f), closely packed AgNPs were formed and well distributed along the CNTs. Further increasing the reaction time to 120s, the density of AgNPs became very high and large agglomerates of AgNPs were observed. By comparing these results, the reaction time of 60s produced the best combination of particle size and AgNP distribution. In the following antimicrobial and toxicity tests, all sphere-shaped AgNPs and AgNP-CNT nano hybrids used were synthesized with the reaction time of 60s.

XRD analysis (Figure 3a) showed that the AgNPs on CNT surfaces was elemental Ag, since the diffraction peaks at  $2\theta$  of  $38.3^\circ$ ,  $44.5^\circ$ ,  $64.6^\circ$ , and  $77.6^\circ$  were from the (111), (200), (220), and (311) crystallographic planes, respectively, of Ag crystal with a face-center-cubic (fcc) symmetry. The peak at  $2\theta$  of  $25.3^\circ$  belonged to CNT-OH. Here,  $\text{AgNO}_3$  was used as a control. The EDX analyses of AgNP-CNT and AgNPs (Figure 3b) further confirmed that elemental Ag was formed on CNTs. The optical absorption peak was centered at 3 keV, which is typical for the absorption of metallic Ag nanocrystals. The Ag content in the AgNP-CNT was  $\sim 22.1\%$ .

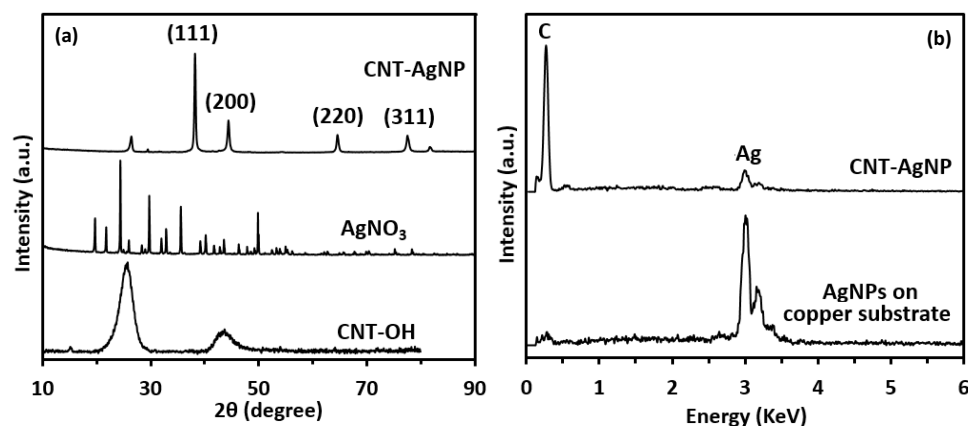


**Figure 3** (a) XRD patterns of CNT-OH, AgNO<sub>3</sub>, and AgNP-CNT. AgNO<sub>3</sub> and CNT-OH were used as controls. (b) EDX spectra of AgNP-CNT and AgNPs on copper substrates.

## Antimicrobial Activity Evaluation and Cell Viability Test

The antimicrobial effect of AgNP-CNT was tested by counting the colony-forming units (CFUs) in three repeated experiments. A clinical strain of *S. aureus* was studied because *S. aureus* was one of the major microorganisms found in bacterial infections. Figure 4a shows a visual result of the antimicrobial effect of AgNP-CNT at various concentrations (0.04–0.8 mM). At 0.8 mM, AgNP-CNT exhibited high antimicrobial activity with no colonies observed. The antimicrobial activities of AgNP-CNT and AgNPs at various concentrations are summarized in Figure 4b. After treating for 30 min, 0.04 mM AgNP-CNT killed 65% of the bacteria, and this value increased to 94% for 0.2 mM AgNP-CNT. When it came to the concentration of 0.4 mM or 0.8 mM, 100% of the bacteria were killed. The antimicrobial activity results of CNTs, AgNPs, and AgNP-CNT at the same molar concentrations (ie, 0.2 mM, 0.4 mM, and 0.8 mM) are summarized in Figure 4c, where synergistically improved antimicrobial properties were observed at both 0.2 mM and 0.4 mM. In

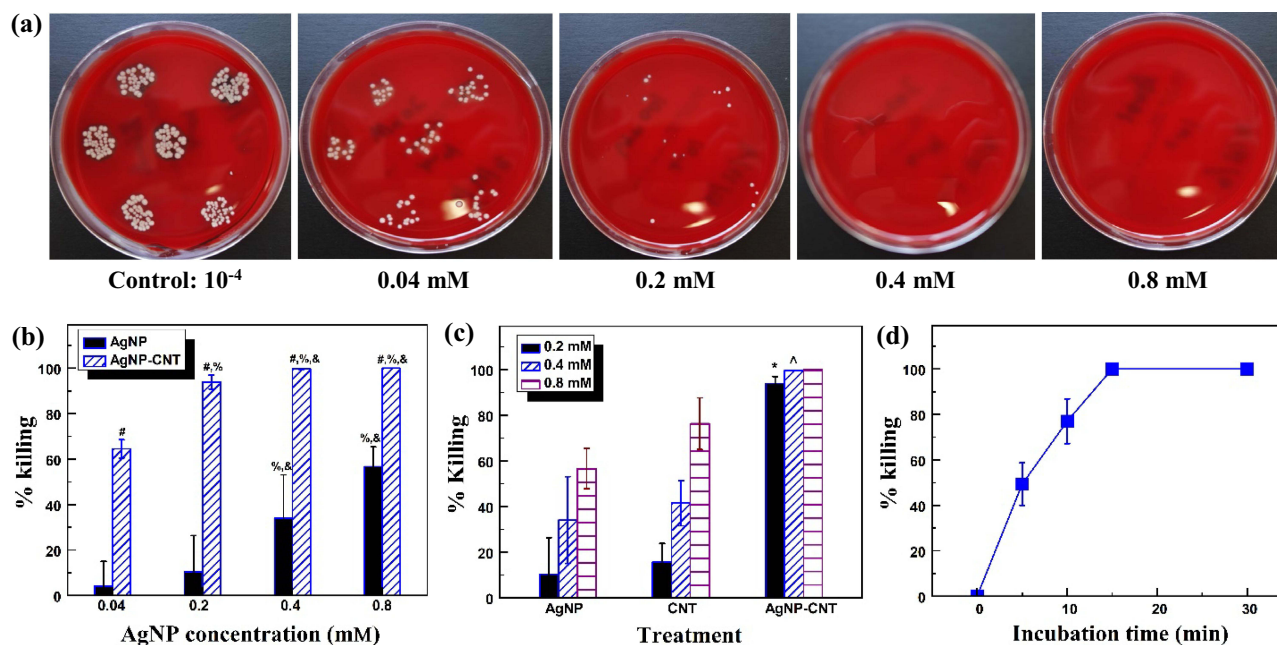


**Figure 4** (a) Visual effects of AgNP-CNT on *S. aureus* killing. (b) Antimicrobial killing percentage of AgNP-CNT and AgNPs against *S. aureus*. (c) Antimicrobial effects of AgNPs, CNTs, and AgNP-CNT at concentrations corresponding to 0.2, 0.4, and 0.8 mM AgNP-CNT. (d) Antimicrobial killing kinetics of AgNP-CNT nanohybrids at 0.2 mM. #Compared to the same concentration of AgNPs, %Compared to the same treatment at 0.04 mM, &Compared to the same treatment at 0.2 mM, \*Synergistically significant when compared to the sum of the treatments of CNTs and AgNPs. p<0.05.

addition, AgNO<sub>3</sub> with the same concentrations (0.2 mM and 0.4 mM) was also tested and compared. AgNO<sub>3</sub> killed 34% and 57% of the bacteria at these two concentrations, respectively, suggesting an advantage of AgNP-CNT over AgNO<sub>3</sub> on bacterial killing.

The kinetics of bacterial killing for AgNP-CNT were also studied. A total volume of 1 mL of solution containing log-phase bacteria ( $3 \times 10^5$  CFU/mL) and AgNP-CNT (200 µg/mL) was used to test the kinetics of AgNP-CNT. The bacterial killing percentage was determined at given time intervals (ie, 5, 10, 15, and 30 min). At the predetermined time, samples including the control were diluted and cultured on blood agar plates using the drop plate method as we previously reported, and CFUs were counted.<sup>17,34</sup> The results of bacterial killing percentage of AgNP-CNT with time are shown in Figure 4d. AgNP-CNT killed approximately half of the *S. aureus* within 5 min and killed almost all of the bacteria within 15 min. Therefore, the killing of *S. aureus* by AgNP-CNT nano hybrids was fast.

Next, we determined the toxicity and biocompatibility of AgNP-CNT nano hybrids toward human cells. The toxicity of CNTs, AgNPs, AgNO<sub>3</sub>, and AgNP-CNT was tested with human osteoblast cells; these tests might allow for the determination of the amount of AgNP-CNT that may be considered non-toxic to humans. We first conducted the cell viability tests of AgNP-CNT and AgNPs with various concentrations that were the same as those studied in Figure 4b. The results are summarized in Figure 5a. The viability of human osteoblast cells decreased with increasing AgNPs and AgNP-CNT concentrations. For all of the concentrations studied, the cell viabilities of human osteoblast cells in the presence of AgNP-CNT were always significantly higher than those in the presence of AgNPs at the same molar concentrations, indicating that hybridizing of AgNPs with CNTs greatly decreased the cytotoxicity of AgNPs. At the 0.4 mM concentration especially, the cell viability for the AgNP-CNT treatment was almost twice that for AgNPs. In addition, our studies showed that, among CNTs, AgNPs, AgNO<sub>3</sub>, and AgNP-CNT, CNTs had the highest and AgNO<sub>3</sub> had the lowest viability of human osteoblast cells (Figure 5b). AgNO<sub>3</sub> killed almost all of the osteoblast cells, indicating its severe toxicity toward osteoblast cells. Ultimately, AgNP-CNT nano hybrids had significantly higher viability of osteoblast cells compared to both AgNPs and AgNO<sub>3</sub> (Figure 5b).

## Discussion

This study focused on the chemical synthesis of AgNP-CNT nano hybrids, and their antimicrobial activity against *S. aureus* and cytotoxicity toward human osteoblast cells. We applied a facile chemical synthesis method to grow AgNPs onto multiwalled CNTs that presented high antimicrobial activity and high human cell viability. The chemical synthesis was based on a traditional silver-mirror reaction; meanwhile, we introduced multiwalled CNTs with abundant functional groups as the carrier for AgNPs. The developed chemical synthesis method made it easy to adjust the size, shape, and distribution of AgNPs on CNTs. Specifically, the shape of AgNPs could be controlled by the amount of chemicals (ie, dextrose) used in the reactions. The chemical synthesis method was fast. The reduction of Ag-ions was clearly visible when adding dextrose aqueous solution into the Tollens reagent and the beaker was covered with a thick

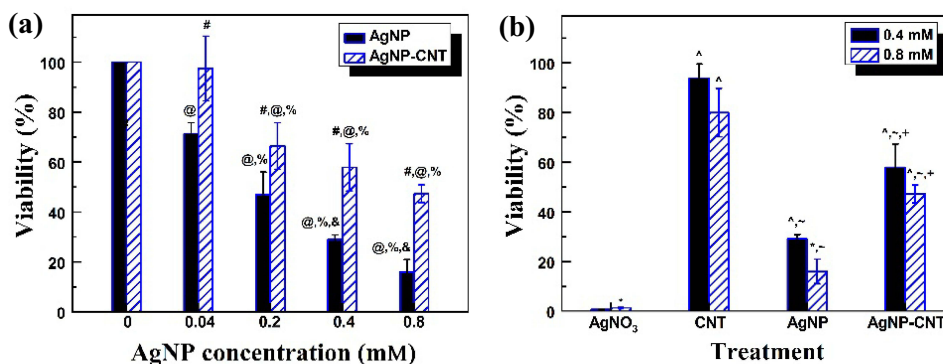


**Figure 5** (a) Osteoblast cell viability of AgNP-CNT and AgNPs at various concentrations. #Compared to the same concentration of AgNPs, @Compared to the corresponding control at concentration of 0, %Compared to the same treatment at 0.04 mM, and &Compared to the same treatment at 0.2 mM. (b) Osteoblast cell viability of AgNPs, CNTs, AgNO<sub>3</sub>, and AgNP-CNT at concentrations corresponding to 0.4 mM and 0.8 mM AgNP-CNT. \*Compared to the same treatment at 0.4 mM, ^Compared to AgNO<sub>3</sub> treatment, ~Compared to CNT treatment, and ~Compared to AgNP treatment. p<0.05.

layer of AgNPs in 30s. The average diameter of AgNPs was as small as 95 nm. CNTs were studied due to the fact that they had high electrical, chemical, mechanical, and thermal stability, and they have often been applied for drug delivery, sensing, diagnostics, anti-inflammatory, anti-angiogenesis, antiviral, and platelet activity.<sup>36</sup> In addition, the high specific surface areas of CNTs might significantly improve the adsorption capacity of AgNPs, while the surface functional groups could lead to well-distributed AgNPs. As a result, AgNPs were found to be uniformly formed on the surfaces of CNTs, which might contribute to high antimicrobial properties. The unique synthesis method also allowed the tuning of the morphologies of AgNPs, and AgNPs of cube, snowflake, and sphere shapes were obtained, making the process amenable to specific application designs.

Ag and its compounds have high antimicrobial properties toward bacteria but, just like other antimicrobial agents, Ag must be used with a certain dosage and application form, and the toxicity (toward host cells) of Ag and its compounds so far has limited their clinical application since they have been reported to cause argyria, hepatopathy, and nephropathy.<sup>37–39</sup> Developing innovative Ag application forms that have high antimicrobial properties and limited toxicity toward hosts will significantly broaden Ag's clinical application. Our findings showed that the toxicity of AgNP-CNT nanohybrids toward human osteoblasts were concentration dependent, while the nanohybrids demonstrated significantly lower toxicity compared to AgNP alone. The AgNP-CNT nanohybrids had excellent osteoblast viability at 0.04 mM and had osteoblast viability at 60% or higher at 0.2 and 0.4 mM. It is noteworthy to mention that, according to the cytotoxicity classification,<sup>40</sup> 60% or higher cell viability is considered non-cytotoxic or slightly toxic.

The advances in nanotechnology that can produce hybrids at the nanometer scale may lead to new findings and renewed interest in Ag's biomedical applications. AgNPs have shown anti-inflammatory and wound healing properties.<sup>41,42</sup> AgNPs induced more rapid healing *in vivo* compared to Ag sulfadiazine treatment and no treatment control, and improved vascularized granulation tissues *in vivo*.<sup>42</sup> AgNPs also presented significantly faster wound closure and reduced scar appearance, in the presence or absence of infections, compared to the treatment of Ag sulfadiazine in a full-thickness excisional wound model in mice.<sup>41</sup> We further hypothesized that nanotechnology may reduce Ag's host toxicity by producing Ag nanohybrids, since nanoparticles have proven to be particularly useful in obtaining sustained drug release and significantly reduced drug dosage (eg, 20 times lower).<sup>43</sup> Nanohybrids of two nanomaterials with different dimensions, such as spherical AgNPs and high-aspect-ratio CNTs, may increase the target-specific antimicrobial capacity while achieving a minimum host toxicity. Silver nanohybrids like AgNP-CNT with high antimicrobial properties and limited host toxicity (Figure 6) may be developed.

In this study, at a concentration of 0.8 mM, AgNPs had a low osteoblast cell viability of 16%, and at the same time, could only kill 57% of the bacteria. Meanwhile, CNTs presented good antimicrobial activity along with excellent osteoblast viability. Hybridizing AgNPs and CNTs has led to synergistically improved antimicrobial properties along with significantly enhanced osteoblast viability compared to AgNPs. For example, at the concentration of 0.4 mM,

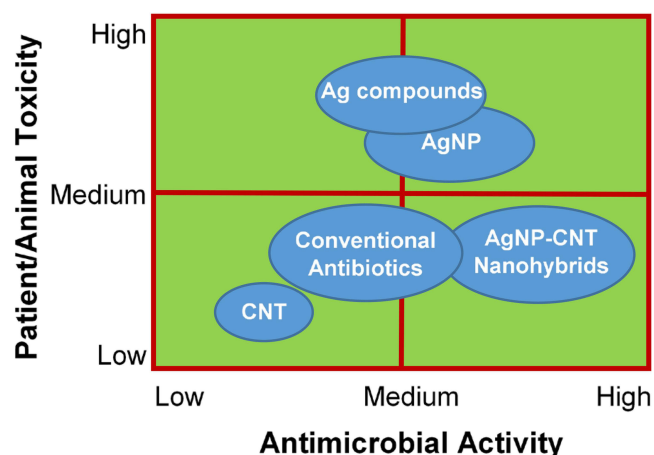


**Figure 6** Ideal antimicrobial and toxicity properties of AgNP-CNT nanohybrids.



AgNP-CNT demonstrated high antimicrobial activity of 100% killing and good osteoblast viability (~60%). This enhanced performance may be attributed to the coordination of interactions between AgNPs and CNTs. The large specific surface area of CNTs provided numerous active sites for AgNPs and greatly decreased their agglomerations; AgNPs are prone to aggregate together and the antimicrobial activity of AgNPs reduces if significant aggregation of AgNPs occurs which leads to reduced active surface areas. Therefore, for the first time, AgNP-CNT nanohybrids with superior antimicrobial and significantly lower host toxicity properties compared to AgNPs were synthesized. Such nanohybrids may increase the target-specific antimicrobial capacity while achieving a minimum host toxicity. As a result, AgNP-CNT nanohybrids may be an innovative antibiotic alternative that can be used to reduce infections while reducing antibiotic resistance. Such nanohybrids will make Ag use much safer and will renew and expand Ag's clinical uses (besides its topical uses).

Besides AgNPs, other metal nanoparticles like cadmium, copper, lead, mercury, nickel, and zinc have also been studied as candidates for antimicrobial applications;<sup>44–46</sup> however, most of them are highly toxic to humans. This study suggests a new nanotechnology-based strategy, hybridizing two antimicrobial nanomaterials with different dimensions, to revive some “old” or new antimicrobial agents (Ag as an example) which currently have limited clinical use due to high host toxicity. These nanohybrids may be applied to significantly improve or revive the therapeutic effectiveness of these metal nanoparticles to make them potentially feasible to treat infectious diseases.

Development of new antimicrobial biomaterials or reformulating old antimicrobial agents has been challenging, and in many cases, a multidisciplinary strategy may be required and new technologies may be needed to fully assess such antimicrobial agents. Meanwhile, infections may be caused by many different pathogens and in many cases, the infection could be polymicrobial (ie, presence of multiple bacteria). Limitations of this study include that only *S. aureus*, one of the major bacteria responsible for orthopaedic infections, was studied. In future work, the effects of the developed nanohybrids may be tested against other bacteria like *Pseudomonas aeruginosa* and *Escherichia coli*. Their effects on polymicrobial infections may also be investigated.

## Conclusions

In summary, we have reported a facile chemical approach to reformulate an old antimicrobial agent for the synthesis of AgNPs with a variety of shapes like cube, snowflake, and sphere on multiwalled CNTs. The AgNP-CNT nanohybrids exhibited excellent antimicrobial properties and high osteoblast cell viability.

## Abbreviations

Ag, silver; AgNO<sub>3</sub>, silver nitrate; AgNPs, silver nanoparticles; AgNP-CNT, nanohybrids of silver nanoparticles and carbon nanotubes; CFUs, colony-forming units; CNTs, carbon nanotubes; DMSO, dimethylsulfoxide; EDX, energy-dispersive X-ray spectroscopy; FBS, fetal bovine serum; H<sub>2</sub>O<sub>2</sub>, hydrogen peroxide; MRSA, methicillin-resistant *Staphylococcus aureus*; NaOH, sodium hydroxide; *S. aureus*, *Staphylococcus aureus*; SEM, scanning electron microscopy; TSB, Tryptic soy broth; XRD, X-ray diffraction.

## Acknowledgments

This work was partially supported by the Office of the Assistant Secretary of Defense for Health Affairs, through the Peer Reviewed Medical Research Program, Discovery Award under Award No. W81XWH1810203. PR acknowledges financial support from West Virginia Higher Education Policy Commission Division of Science and Research. The authors also acknowledge the use of the WVU Shared Research Facilities. Opinions, interpretations, conclusions, and recommendations are those of the authors and are not necessarily endorsed by the funding agencies. The authors acknowledge Professor Gerald R. Hobbs at WVU for help with data analysis and Suzanne Danley for proofreading.

## Supplementary Materials

Data on the characterization of CNTs can be found in the [Supplementary Information](#).

## Disclosure

The authors declare no conflict of interest. The funders had no role in the design of the study; in the collection, analyses, or interpretation of data; in the writing of the manuscript, or in the decision to publish the results.

## References

1. Li B, Webster TJ. Bacteria antibiotic resistance: new challenges and opportunities for implant-associated orthopedic infections. *J Orthop Res*. 2018;36(1):22–32. doi:10.1002/jor.23656
2. Friedman ND, Temkin E, Carmeli Y. The negative impact of antibiotic resistance. *Clin Microbiol Infect*. 2016;22(5):416–422. doi:10.1016/j.cmi.2015.12.002
3. Teillant A, Gandra S, Barter D, Morgan DJ, Laxminarayan R. Potential burden of antibiotic resistance on surgery and cancer chemotherapy antibiotic prophylaxis in the USA: a literature review and modelling study. *Lancet Infect Dis*. 2015;15(12):1429–1437. doi:10.1016/S1473-3099(15)00270-4
4. Mainous AG 3rd, Diaz VA, Matheson EM, Gregorie SH, Hueston WJ. Trends in hospitalizations with antibiotic-resistant infections: US, 1997–2006. *Public Health Rep*. 2011;126(3):354–360. doi:10.1177/003335491112600309
5. Centers for Disease Control and Prevention. Antibiotic resistance threats in the United States; 2019. Available from: <https://www.cdc.gov/drugresistance/pdf/threats-report/2019-ar-threats-report-508.pdf/>. Accessed January 16, 2023.
6. Boucher HW, Talbot GH, Benjamin DK Jr, et al. 10 x '20 progress—development of new drugs active against gram-negative bacilli: an update from the infectious diseases society of America. *Clin Infect Dis*. 2013;56(12):1685–1694. doi:10.1093/cid/cit152
7. Mirsattari SM, Hammond RR, Sharpe MD, Leung FY, Young GB. Myoclonic status epilepticus following repeated oral ingestion of colloidal silver. *Neurology*. 2004;62(8):1408–1410. doi:10.1212/01.WNL.0000120671.73335.EC
8. Alt V, Bechert T, Steinrucke P, et al. An in vitro assessment of the antibacterial properties and cytotoxicity of nanoparticulate silver bone cement. *Biomaterials*. 2004;25(18):4383–4391. doi:10.1016/j.biomaterials.2003.10.078
9. Honda M, Kawanobe Y, Ishii K, et al. In vitro and in vivo antimicrobial properties of silver-containing hydroxyapatite prepared via ultrasonic spray pyrolysis route. *Mater Sci Eng C Mater Biol Appl*. 2013;33(8):5008–5018. doi:10.1016/j.msec.2013.08.026
10. Morones-Ramirez JR, Winkler JA, Spina CS, Collins JJ. Silver enhances antibiotic activity against gram-negative bacteria. *Sci Transl Med*. 2013;5(190):190ra81. doi:10.1126/scitranslmed.3006276
11. Elashnikov R, Lyutakov O, Kalachyova Y, Solovyev A, Svorcik V. Tunable release of silver nanoparticles from temperature-responsive polymer blends. *React Funct Polym*. 2015;93:163–169. doi:10.1016/j.reactfunctpolym.2015.06.010
12. Ahmed B, Hashmi A, Khan MS, Musarrat J. ROS mediated destruction of cell membrane, growth and biofilms of human bacterial pathogens by stable metallic AgNPs functionalized from bell pepper extract and quercetin. *Adv Powder Technol*. 2018;29(7):1601–1616. doi:10.1016/j.apt.2018.03.025
13. Elashnikov R, Radocha M, Panov I, et al. Porphyrin-silver nanoparticles hybrids: synthesis, characterization and antibacterial activity. *Mater Sci Eng C*. 2019;102:192–199. doi:10.1016/j.msec.2019.04.029
14. Rani P, Ahmed B, Singh J, et al. Silver nanostructures prepared via novel green approach as an effective platform for biological and environmental applications. *Saudi J Biol Sci*. 2022;29(6):103296. doi:10.1016/j.sjbs.2022.103296
15. Chauhan V, Dhiman VK, Mahajan G, Pandey A, Kanwar SS. Synthesis and characterization of silver nanoparticles developed using a novel lipopeptide (s) biosurfactant and evaluating its antimicrobial and cytotoxic efficacy. *Proc Biochem*. 2023;124:51–62. doi:10.1016/j.procbio.2022.11.002
16. Kannan K, Govindaraj M, Rajeswari B, Vijayakumar K. Green synthesis silver nanoparticles using medicinal plant and antimicrobial activity against human pathogens. *Mater Today Proc*. 2022;69:1346–1350. doi:10.1016/j.matpr.2022.08.506
17. Kang J, Dietz MJ, Hughes K, Xing M, Li B. Silver nanoparticles present high intracellular and extracellular killing against *Staphylococcus aureus*. *J Antimicrob Chemother*. 2019;74(6):1578–1585. doi:10.1093/jac/dkz053
18. Kang J, Dietz MJ, Li B. Antimicrobial peptide LL-37 is bactericidal against *Staphylococcus aureus* biofilms. *PLoS One*. 2019;14(6):e0216676. doi:10.1371/journal.pone.0216676
19. Silver S, Phung LT, Silver G. Silver as biocides in burn and wound dressings and bacterial resistance to silver compounds. *J Ind Microbiol Biotechnol*. 2006;33(7):627–634. doi:10.1007/s10295-006-0139-7
20. Silver S. Bacterial silver resistance: molecular biology and uses and misuses of silver compounds. *FEMS Microbiol Rev*. 2003;27(2–3):341–353. doi:10.1016/S0168-6445(03)00047-0
21. Bragg P, Rainnie D. The effect of silver ions on the respiratory chain of *Escherichia coli*. *Can J Microbiol*. 1974;20(6):883–889. doi:10.1139/m74-135
22. Randall CP, Oyama LB, Bostock JM, Chopra I, O'Neill AJ. The silver cation (Ag<sup>+</sup>): antistaphylococcal activity, mode of action and resistance studies. *J Antimicrob Chemother*. 2013;68(1):131–138. doi:10.1093/jac/dks372
23. Russell A, Hugo W. 7 antimicrobial activity and action of silver. *Progr Med Chem*. 1994;31:351–370.
24. Oluwalowo A, Nguyen N, Zhang S, Park JG, Liang R. Electrical and thermal conductivity improvement of carbon nanotube and silver composites. *Carbon*. 2019;146:224–231. doi:10.1016/j.carbon.2019.01.073
25. Zhao S, Li J, Cao D, et al. Percolation threshold-inspired design of hierarchical multiscale hybrid architectures based on carbon nanotubes and silver nanoparticles for stretchable and printable electronics. *J Mater Chem C*. 2016;4(27):6666–6674. doi:10.1039/C6TC01728B
26. Takei K, Yu Z, Zheng M, Ota H, Takahashi T, Javey A. Highly sensitive electronic whiskers based on patterned carbon nanotube and silver nanoparticle composite films. *Proc Natl Acad Sci*. 2014;111(5):1703–1707. doi:10.1073/pnas.1317920111
27. Ahmadpoor F, Zebarjad SM, Janghorban K. Decoration of multi-walled carbon nanotubes with silver nanoparticles and investigation on its colloid stability. *Mater Chem Phys*. 2013;139(1):113–117. doi:10.1016/j.matchemphys.2012.12.071
28. Prodana M, Ionita D, Ungureanu C, Bojin D, Demetrescu I. Enhancing antibacterial effect of multiwalled carbon nanotubes using silver nanoparticles. *Microscopy*. 2011;6(2):549–556.
29. Fortunati E, D'angelo F, Martino S, Orlacchio A, Kenny J, Armentano I. Carbon nanotubes and silver nanoparticles for multifunctional conductive biopolymer composites. *Carbon*. 2011;49(7):2370–2379. doi:10.1016/j.carbon.2011.02.004

30. Chun K-Y, Oh Y, Rho J, et al. Highly conductive, printable and stretchable composite films of carbon nanotubes and silver. *Nat Nanotechnol.* 2010;5(12):853–857. doi:10.1038/nnano.2010.232
31. Feng Y, Yuan H. Electroless plating of carbon nanotubes with silver. *J Mater Sci.* 2004;39(9):3241–3243. doi:10.1023/B:JMSE.0000025869.05546.94
32. Yan J, Liu X, Qi H, et al. High-performance lithium–sulfur batteries with a cost-effective carbon paper electrode and high sulfur-loading. *Chem Mater.* 2015;27(18):6394–6401. doi:10.1021/acs.chemmater.5b02533
33. Yan J, Liu X, Yao M, Wang X, Wafle TK, Li B. Long-life, high-efficiency lithium–sulfur battery from a nanoassembled cathode. *Chem Mater.* 2015;27(14):5080–5087. doi:10.1021/acs.chemmater.5b01780
34. Noore J, Noore A, Li B. Cationic antimicrobial peptide LL-37 is effective against both extra- and intracellular *Staphylococcus aureus*. *Antimicrob Agent Chemother.* 2013;57(3):1283–1290. doi:10.1128/AAC.01650-12
35. Armstead AL, Simoes TA, Wang X, et al. Toxicity and oxidative stress responses induced by nano- and micro-CoCrMo particles. *J Mater Chem B.* 2017;5(28):5648–5657. doi:10.1039/C7TB01372H
36. Santos CM, Tria MCR, Vergara RAMV, Ahmed F, Advincula RC, Rodrigues DF. Antimicrobial graphene polymer (PVK-GO) nanocomposite films. *Chem Commun.* 2011;47(31):8892–8894. doi:10.1039/c1cc11877c
37. Trop M, Novak M, Rodl S, Hellbom B, Kroell W, Goessler W. Silver-coated dressing acticoat caused raised liver enzymes and argyria-like symptoms in burn patient. *J Trauma.* 2006;60(3):648–652. doi:10.1097/01.ta.0000208126.22089.b6
38. Bouts BA. Images in clinical medicine. Argyria. *N Engl J Med.* 1999;340(20):1554. doi:10.1056/NEJM199905203402006
39. Hollinger MA. Toxicological aspects of topical silver pharmaceuticals. *Crit Rev Toxicol.* 1996;26(3):255–260. doi:10.3109/10408449609012524
40. Kong N, Jiang T, Zhou Z, Fu J. Cytotoxicity of polymerized resin cements on human dental pulp cells in vitro. *Dent Mater.* 2009;25(11):1371–1375. doi:10.1016/j.dental.2009.06.008
41. Liu X, Lee PY, Ho CM, et al. Silver nanoparticles mediate differential responses in keratinocytes and fibroblasts during skin wound healing. *ChemMedChem.* 2010;5(3):468–475. doi:10.1002/cmde.200900502
42. Wright JB, Lam K, Buret AG, Olson ME, Burrell RE. Early healing events in a porcine model of contaminated wounds: effects of nanocrystalline silver on matrix metalloproteinases, cell apoptosis, and healing. *Wound Repair Regen.* 2002;10(3):141–151. doi:10.1046/j.1524-475X.2002.10308.x
43. Shah PN, Lin LY, Smolen JA, et al. Synthesis, characterization, and in vivo efficacy of shell cross-linked nanoparticle formulations carrying silver antimicrobials as aerosolized therapeutics. *ACS Nano.* 2013;7(6):4977–4987. doi:10.1021/nn400322f
44. Čík G, Bujdaková H, Šeršeň F. Study of fungicidal and antibacterial effect of the Cu (II)-complexes of thiophene oligomers synthesized in ZSM-5 zeolite channels. *Chemosphere.* 2001;44(3):313–319. doi:10.1016/S0045-6535(00)00306-4
45. Ulküseven B, Tavman A, Otük G, Birteksöz S. Antimicrobial activity of FeIII, CuII, AgI, ZnII and HgII complexes of 2-(2-hydroxy-5-bromo/nitrophenyl)-1H- and 2-(2-hydroxyphenyl)-5-methylchloro/nitro-1H-benzimidazoles. *Folia Microbiol.* 2002;47(5):481–487. doi:10.1007/BF02818785
46. Chohan ZH, Supuran CT, Scozzafava A. Metalloantibiotics: synthesis and antibacterial activity of cobalt (II), copper (II), nickel (II) and zinc (II) complexes of kefzol. *J Enzyme Inhib Med Chem.* 2004;19(1):79–84. doi:10.1080/14756360310001624939

International Journal of Nanomedicine

Dovepress

## Publish your work in this journal

The International Journal of Nanomedicine is an international, peer-reviewed journal focusing on the application of nanotechnology in diagnostics, therapeutics, and drug delivery systems throughout the biomedical field. This journal is indexed on PubMed Central, MedLine, CAS, SciSearch®, Current Contents®/Clinical Medicine, Journal Citation Reports/Science Edition, EMBASE, Scopus and the Elsevier Bibliographic databases. The manuscript management system is completely online and includes a very quick and fair peer-review system, which is all easy to use. Visit <http://www.dovepress.com/testimonials.php> to read real quotes from published authors.

Submit your manuscript here: <https://www.dovepress.com/international-journal-of-nanomedicine-journal>